# In Situ ATR−FTIR Investigation on the Preparation and Enantiospecificity of Chiral Polyelectrolyte Multilayers

**ARTICLE** *in* ACS APPLIED MATERIALS & INTERFACES · DECEMBER 2009

Impact Factor: 6.72 · DOI: 10.1021/am900597c · Source: PubMed



**4 AUTHORS**, INCLUDING:

Martin Müller
Leibniz Institute of Polymer Research Dres…
**127** PUBLICATIONS **1,792** CITATIONS
SEE PROFILE

Brigitte Voit
Leibniz Institute of Polymer Research Dres…
**343** PUBLICATIONS **4,179** CITATIONS
SEE PROFILE

ARTICLE

# In Situ ATR-FTIR Investigation on the Preparation and Enantiospecificity of Chiral Polyelectrolyte Multilayers

**Wuye Ouyang, Martin Müller,* Dietmar Appelhans, and Brigitte Voit**

Leibniz-Institute of Polymer Research Dresden eV (IPF), Hohe Strasse 6, 01069 Dresden, Germany

**ABSTRACT** Chiral polyelectrolyte multilayers (PEMs) consisting of poly(L-lysine) (PLL), poly(*N*-(S)alkylated 4-vinylpyridinium iodide), or poly(ethyleneimine maltose) (PEI-m) as polycations and poly(styrenesulfonic acid) sodium salt (PSS) or poly(vinyl sulfate) as polyanions, as well as a nonchiral PEM composed of poly(ethyleneimine) (PEI) and PSS were deposited on silicon substrates and poly(tetrafluoroethylene) membranes using the layer-by-layer method. For these PEMs, enantiospecific interaction toward one enantiomer of either L/D-glutamic acid (L/D-GLU), L/D-tryptophan, or L/D-ascorbic acid (L/D-ASC), respectively, was studied under variation of the concentration, pH, and ionic strength. Both deposition and enantiospecific interaction were analyzed by attenuated total reflection Fourier transform infrared spectroscopy. Our results show a significant enantiospecific preference of D-GLU over L-GLU at PEMs containing PLL and of D-ASC over L-ASC at PEMs containing PEI-m. No such enantiospecific preference was found for nonchiral PEMs containing PEI. The enantiospecificity of PEMs of PLL/PSS toward L/D-GLU could be significantly influenced by the ionic strength and pH values, so that increasing attractive electrostatic interactions resulted in higher enantiospecificity.

**KEYWORDS:** chiral surface • polyelectrolyte multilayer • enantiospecific interaction • amino acids • ascorbic acid • permeation

## INTRODUCTION

Enantiospecific surfaces are able to bind one enantiomer (e.g., the L form) of a chiral substance to a higher extent than the other one (e.g., the D form), which is originated in the chiral nature of the surface forming (macro)molecules. Enantiospecific surfaces and layers play an important role for the analytical recognition and preparative separation of chiral drugs in the pharmaceutical industry (1, 2). Most prominent in that respect is the coating of stationary phases used for HPLC by a chiral selector (SO), which can be a chiral reactive polymer or low-molecular compound. An example for low-molecular chiral SO is (*R*)-(−)-*N*-(3,5-dinitrobenzoyl)phenylglycin (Chirasep) on aminated silica gel ("Pirkle phase" (3))4, 5), and one for the polymer-based chiral SO is poly(*N*-acryloyl-L-phenylalanin ethyl ester) bound to silica gel (Chiraspher (5)). Weak interactions like $\pi-\pi$, dipole−dipole, and hydrogen-bonding acting via at least three centers are generally claimed to contribute to the enantiospecific recognition (6) between a chiral probe and the chiral SO. However, because such chiral stationary phases are very expensive, alternatives are sought. In that framework, a further possible concept for enantiospecific recognition is based on molecular imprinting of a chiral probe in a sol/gel matrix (7), possessing cavities with high steric specifity. Related to that, Kaner et al. reported high enantiospecificity of casted polyaniline films toward L-phenylalanine over D-phenylalanine, exclusively after chiral doting with (*R*)-camphorsulfonic acid (8, 9). Up to now, the concept of polyelectrolyte multilayers (PEMs) for the generation of chiral surfaces was considered only to a low extent. Solely, Rmaile and Schlenoff (10) reported studies on thick PEM membranes consisting of oppositely charged chiral polyelectrolytes (PEL) for the separation of small chiral probes like L- and D-ascorbic acid (L/D-ASC). Low-percent-selectivity values (see eq 4) of around 3% were obtained by attenuated total reflection Fourier transform infrared (ATR-FTIR) spectroscopy and capillary electrochromatography.

Herein, we report on the results of related studies using PEMs consisting of charged polypeptides and synthetic chiral PELs as chiral SO for enantiospecific binding of L/D-glutamic acid (L/D-GLU) and L/D-ASC as chiral probes. A specific aim of this work is dedicated to the influence of an aqueous medium and the PEL type within PEMs on enantiospecificity. In situ ATR-FTIR spectroscopy was used as a powerful tool for the characterization of PEM and PEM interaction, which has been shown also by Granick (11, 12), Schaaf (13−16), Sukhishvili (17−19) and Schlenoff (20−22). In our group, it was successfully used to characterize the deposition (23), molecular composition (24), conformation, and orientation within PEMs (25, 26) as well as the binding of small ions (27), surfactants (28), and proteins (23, 29, 30) on a quantitative level.

## EXPERIMENTAL SECTION

**PELs, Chiral Probes, and Substrates.** Poly(L-lysine) (PLL; $M_w$ = 280 000 g/mol) and branched poly(ethylenemine) (PEI; $M_w$ = 750 000 g/mol) were obtained from Sigma Aldrich (Deisenhofen, Germany), and poly(styrenesulfonic acid) sodium salt (PSS; $M_w$ = 70 000 g/mol) was obtained from Polysciences, Inc. (Warrington, PA). Poly(vinyl sulfate) (PVS; $M_w$ = 300 000 g/mol) was obtained from Gelest, Inc. (Morrisville, PA). Poly(ethyleneimine maltose) (PEI-m) was received by the reductive amination

* E-mail: mamuller@ipfdd.de.

Received for review September 2, 2009 and accepted November 9, 2009

DOI: 10.1021/am900597c





Published on Web 11/23/2009

of branched PEI in the presence of excess maltose using a slightly modified method described in the literature (31); the degree of substitution of PEI with maltose is higher than 70%. Poly(*N*-(S)alkylated-4-vinylpyridinium iodide) (PVP-R) was synthesized according to the literature (10). L/D-Glutamic acid (L/D-GLU), L/D-ascorbic acid (L/D-ASC), and L/D-tryptophan (L/D-TRP) were obtained from Sigma Aldrich (Deisenhofen, Germany). All commercial samples were used without further purification. PEI, PLL, PSS, and PVS were dissolved in Millipore water at $c_{PEL} = 0.005$ M. PVP-R was dissolved in a 0.1 M NaCl solution at $c_{PVP\text{-}R} = 0.5$ mg/mL. PEI-m was dissolved in Millipore water at $c_{PEI\text{-}m} = 0.5$ mg/mL. L- and D-GLU were dissolved in Millipore water at different concentrations of $c_{GLU}$. HCl (1 M) and NaOH (1 M) were used to adjust the pH value of PEL and GLU solutions. L- and D-ASC were dissolved in Millipore water at a concentration of $c_{ASC} = 0.05$ M and pH = 4.0 (adjusted by 1 M NaOH). L- and D-TRP were dissolved in Millipore water at a concentration of $c_{TRP} = 0.05$ M.

Silicon or germanium internal reflection elements (Si- or Ge-IRE) were used as substrates. The Si-IRE was cleaned with a piranha solution [$H_2SO_4$:$H_2O_2$ = 3:1 (v/v)] for 30 min, thoroughly rinsed by water, dried under $N_2$, and finally placed in a plasma cleaner (PDC-32 G plasma cleaner/sterilizer, Harrick, Ossining, NY) for 30 min. The Ge-IRE was cleaned only by Millipore water and a plasma cleaner for 30 min. Then the clean Si/Ge-IRE was fixed in the ATR-FTIR in situ cell (which will be described in the ATR-FTIR section) for recording respective ATR-FTIR spectra.

**Multilayer Deposition on IREs.** The PEM deposition procedure was performed using the stream coating technique, which is based on the classical dipping technique of the layer-by-layer (LBL) concept (32). The deposition procedure is given in detail in the following: polycation solutions (PLL, PEI, PEI-m, and PVP-R) and polyanion solutions (PSS and PVS) were consecutively injected, keeping a final volume of 100 $\mu$L for 10 min above the Si/Ge-IRE in the sample compartment of the ATR-FTIR in situ cell. The solvent was kept in the reference compartment of the ATR-FTIR in situ cell. After each adsorption step, the sample compartment was rinsed by the solvent. All of the PEL solutions and the solvent were circulated by a peristaltic pump at a speed of 3 mL/min for 20 s and 1 min, respectively. For PEMs containing PLL, PEI, and PEI-m, after the final odd PEM adsorption step, a glutardialdehyde solution [0.25% (w/w)] was immersed to cross-link free amine groups and stabilize the PEMs.

**Enantiospecific Interaction.** For PEM-PLL/PSS, the L/D-GLU concentration was varied in the range $c_{GLU} = 0.0012-0.05$ M. Additionally, 0.05 M L/D-GLU solutions with pH = 2.5−7 or with NaCl concentrations $c_{NaCl} = 0.001-0.1$ M were prepared to investigate the influence of an aqueous medium on enantiospecificity. L/D-GLU solutions were immersed above the PEM film, starting with the lowest $c_{GLU}$, pH, or $c_{NaCl}$, followed by rinsing with pure Millipore water and then immersion of the solution with the next higher $c_{GLU}$, pH, or $c_{NaCl}$ setting, followed again by rinsing. The L/D-GLU solutions were kept in the sample compartment for 20 min. For repetitions of the chiral probe binding series on the same PEM film, a 1 M NaCl solution was used to release the bound chiral probes. For other PEM systems, $c_{GLU}$ was 0.05 M at pH = 3.25 and $c_{ASC}$ was 0.05 M at pH = 4.0.

For a quantitative evaluation of the enantiospecific interaction, the percent of enantiospecificity ($S_E$) was determined according to eq 1, as was used and differently termed therein (10):

$$S_E = \frac{\Gamma_{D(L)} - \Gamma_{L(D)}}{\Gamma_{D(L)}} \times 100\% \quad (1)$$

$\Gamma_L$ and $\Gamma_D$ are the surface concentrations of bound L and D enantiomers. As an approximation, instead of $\Gamma_L$ and $\Gamma_D$, the band integrals $A_L$ and $A_D$ of bound chiral probes can be used for thin PEM films.

**Membrane Modification and Enantiospecific Permeation.** Permeability measurements were carried out for L/D-TRP through a PEM-PLL/PSS-modified poly(tetrafluoroethylene) membrane (PTFE; pore size 0.2 $\mu$m, Sigma Aldrich) immersed in aqueous ethanol by using a two-compartment glass tube at room temperature. To deposit PEM on the membranes, the membrane was first treated by a plasma cleaner for 30 min and then immersed in the experimental solvents (75 vol % ethanol/$H_2O$) for 1 h. PLL and PSS with 0.005 M were consecutively deposited on the membrane by dip-coating. After the final layer adsorption, glutardialdehyde (0.25 wt %) was used to stabilize the PEM.The membrane was placed in the center of the permeation cell with O-rings on either side of the membrane. The upstream and downstream compartments of the permeation tube contained 50 mL of a 0.0005 M L/D-TRP solution and the solvent, respectively. Both the solution and solvent were magnetically stirred to minimize stagnant boundary layers on the membrane surfaces. At each sampling interval, 1 mL of the downstream solution was taken out and 1 mL of the fresh solvent was refilled. The amount of L/D-TRP in the downstream was determined by an UV−vis spectrophotometer (GetSpec-2048, Dresden, Germany) at 280 nm.

The flux $J$ (mol/cm$^2 \cdot$ s) through the membrane can be calculated by

$$J = \frac{\Delta C V}{\Delta t A} \quad (2)$$

where $\Delta C$ is the change in the concentration, $\Delta t$ is the permeation time, $V$ is the downstream volume, and $A$ is the effective membrane area (2.83 cm$^2$). The permeability coefficient $P$ (cm$^2$/s) is given by

$$P = \frac{Jd}{C_u - C_d} \quad (3)$$

where $d$ is the membrane thickness and $C_u$ and $C_d$ are the concentrations of the upstream and downstream. The enantiospecificity was calculated according to the ratio of the permeability coefficients ($P_L$ or $P_D$) for the two enantiomers.

**ATR-FTIR.** Both consecutive PEL deposition and enantiospecific adsorption were characterized by in situ ATR-FTIR spectroscopy using a commercial ATR-FTIR mirror attachment operated by the single-beam-sample-reference (SBSR) concept (Optispec, Zürich, Switzerland). The ATR-FTIR mirror attachment was installed on an IFS 55 Equinox FTIR spectrometer (Bruker Optics GmbH, Ettlingen, Germany) equipped with a globar source and a mercury−cadmium−telluride (MCT) detector. A home-built transparent in situ cell (MM, IPF, Dresden, Germany) was used, which sealed a silicon (Si) or germanium (Ge) crystal by oval O-rings, forming an upper sample (S), which can be filled with the PEL or chiral probe solution, and a lower reference (R) compartment, which can be filled with the solvent. The SBSR concept implies that single-channel spectra $I_{S,R}$ were recorded of both the upper (S) and lower (R) half/compartment of the Si/Ge-IRE (50 × 20 × 2 mm$^3$) by one IR beam. Normalizing the single-channel spectra according to SBSR [$A(\nu) = -\log(I_S(\nu)/I_R(\nu)$] resulted in absorbance spectra [$A(\nu)$] with proper compensation of the background absorptions due to the IRE material, solvent, water vapor (spectrometer), and ice on the MCT detector window.

**ATR-FTIR Analysis.** The quantitative ATR-FTIR analysis is based on a modified Lambert−Beer law (eq 4):

$$A = N\varepsilon c d_e \quad (4)$$

where $A$ is the integral of a characteristic IR band, $N$ is the number of reflections, $\varepsilon$ is the absorption coefficient, $c$ is the concentration of the analyte, which is related to the surface concentration $\Gamma$ by multiplication with the thickness of the

coating layer $d$, and $d_e$ is the effective thickness, which is a function of the evanescent electrical field amplitude, the depth of penetration $d_p$, the thickness $d$, and refractive indices (33). The effective thickness $d_e$ is given by eq 5:

$$d_e = \frac{n_3 d_p E^2}{2 \cos\theta n_1}\left[\exp\left(-2\frac{z_1}{d_p}\right) - \exp\left(-2\frac{z_2}{d_p}\right)\right] \quad (5)$$

where $n_3$ is the reflection index of the polymer layer (PEM), $\theta$ is the incident angle, $E$ is the relative electrical field, and $z_1$ and $z_2$ are the starting and ending positions of the probed PEM zone. In PEM deposition, $z_1 = 0$ and $z_2$ is the thicknesses of PEMs ($d$).

The penetration depth ($d_p$) is the distance $z$, where the electrical field amplitude at $z = 0$ has decayed to a value multiplied by a factor of $1/e$. $d_p$ is a function of the incident angle, involved refractive indices (33), and is given in eq 6:

$$d_p = \frac{\lambda}{2\pi n_1(\sin\theta^2 - n_{21}^2)^{1/2}} \quad (6)$$

where $\lambda$ is the wavelength of light propagating through the rare medium, $n_1$ is the refractive index of the rare medium, and $n_{21}$ is the ratio of refractive indices of the rare medium to the dense medium. In this work, only the Si-IRE was used as the substrate for enantiospecific interaction, and then the penetration depth ranged around $d_p \approx 460$ nm (Si-IRE/$H_2O$). When eqs 4−6 are combined, a functional relationship between $A$ and $d$ can be obtained. The course of $A(d)$ is due to a $1 - \exp(-d/d_p)$ type of function, so that $A$ approaches a constant value with increasing $d$ and thus the ATR-FTIR method gets increasingly insensitive to outer film regions with an increase in the film thickness $d$. However, from $d = 0$−300 nm, a linear relationship between $A$ and $d$ can be approximated.

Using ATR-FTIR for the analysis of enantiospecific adsorption from higher concentrated chiral probe solutions, the spectral contribution from the bulk solution must be considered. Because of the property of the evanescent wave, the contribution of the bulk GLU solution on the total GLU band integral for thick PEM is smaller compared to that for thin PEM. According to eq 1, if the contribution of band integral due to bulk GLU solution (the band integral for 0.05 M GLU in contact with naked Si-IRE is approximately 0.6 $cm^{-1}$) had been subtracted from the total GLU band integral, the enantiospecificity $S_E$ value for all PEMs would be enlarged with a different scale. However, thin films must be scaled to a larger degree than thick films because the spectral contribution of the bulk solution above thin films plays a more dominant role. Therefore, a scaling factor SF is introduced for evaluation of the integrals proportional to the "true" adsorbed amount of enantiomers ($A_{BOUND}$). The integrals of IR bands due to bound enantiomers are obtained according to the following equation:

$$A_{BOUND} = A_{ORIG} - SF \times A_{BULK} \quad (7)$$

where $A_{ORIG}$ is the band integral obtained directly from ATR-FTIR, including bulk and bound GLU contributions and $A_{BULK}$ is the band integral due to the bulk enantiomer solution in contact with naked Si-IRE. The scaling factor SF is calculated by comparing the effective thicknesses ($d_e$) for the bulk enantiomer solution in contact with naked Si-IRE ($z_1 = 0$) and with PEMs ($z_1 \geq 0$) based on the modified Lambert−Beer law (eq 4). The two limiting values are SF = 1, which is due to no PEM layer or a PEM layer that is ideally permeable for the analyte solution and the full subtraction of $A_{BULK}$, and SF = 0, which is due to a thick PEM layer and no subtraction of $A_{BULK}$. Therefore, in principle, SF = 1 for $d_e$ ($z_1 = 0$) and SF = 0 for $d_e$ ($z_1$ = infinity) are set. For clarification, a plot of SF vs $z_1$ is shown in Figure 1.

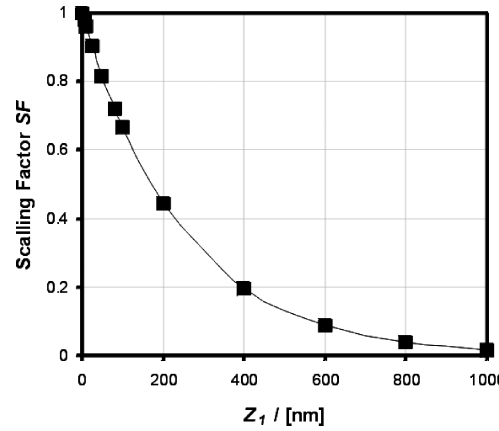


**FIGURE 1. Relationship between the scaling factor SF and the position $z_1$.**

From Figure 1, it can be found that even for the thickest chiral PEM films used in this work (∼40 nm) scaling factors of SF > 0.81 have to be used to get the "true" band integrals directly related to bound GLU. In other words, in the extreme case when the PEM films were highly porous (the "true" $z_1$ is smaller), so that GLU molecules from the bulk solution may freely approach the IRE surface, a value of SF = 1 would be justified. Hence, knowing that one cannot give exact values for a "true" PEM thickness value $d = z_1$, SF values must in all cases exceed 0.81. Of course, this strongly influences the $S_E$ ($S_E = A_D - A_L/A_D$) values of this study. Therefore, in Table 1, in addition to the values of $S_E$, also those of thickness $d$ are given, which result in scaling factors of SF > 0.81.

## RESULTS AND DISCUSSION

Herein, we report on the deposition of enantiospecific PEMs, which were formed by consecutive adsorption of the chiral polycations PLL, PEI-m, and PVP-R and the polyanions PSS and PVS. Additionally, a nonchiral PEM of PEI and PSS was also prepared and used for comparison to enantiospecific interaction of the chiral PEMs. Enantiospecificity $S_E$ was checked by interaction of these PEMs with L/D-GLU and L/D-ASC, respectively, as chiral probes.

In the following, first, in situ ATR-FTIR results upon PEM deposition will be described and, second, their enantiospecific interaction will be treated. In the end, application-oriented results of enantiospecific permeation experiments using a PEM-modified porous PTFE membrane is illustrated.

**1. PEM Deposition.** In the following, deposition data on PEMs consisting of chiral and nonchiral PELs are given. Generally, for these systems, preparation conditions were chosen, enabling the most effective deposition, i.e., the largest increase in the deposited amount with the smallest number of adsorption steps $z$.

In Figure 2, in situ ATR-FTIR spectra on the deposition of PEM-PLL/PSS-$z$ under pH = 10 conditions are shown with increasing adsorption step $z = 1$− 9 from bottom to top. Increasing signals of the amide I band (1648 $cm^{-1}$), amide II band (1545 $cm^{-1}$), and $\nu(SO_2)$ band (1206 $cm^{-1}$) are visible with increasing $z$, which are due to the peptide group of PLL and the sulfate group of PSS. The $\nu$(OH) band (3300 $cm^{-1}$) from $H_2O$ decreased with increasing adsorption steps, which is due to the replacement of $H_2O$ molecules from the Ge-IRE surface by deposited PEM. In principle, these band

**Table 1. Integrals of $\nu(SO_2)$ and Thicknesses (Dry State) (37) of Studied PEM Systems and Their Corresponding Percent Enantiospecificities Related to L/D-GLU and L/D-ASC Binding**

| PEM | $\mathbf{A}_{\nu(SO_2)}$ [$cm^{-1}$] | thickness [nm] | GLU (0.05 M) [%] | ASC (0.05 M) [%] |
|---|---|---|---|---|
| PEM-9-PEI/PSS | 1.57 | 12 | 0 | 0 |
| PEM-9-PLL/PSS | 1.15 | 15 | 21 ± 5 (D > L) | 11 ± 5 (D > L) |
| PEM-9-PVP-R/PSS | 0.80 | 18 | 2 ± 1 (D > L) | 5 ± 1 (D > L) |
| PEM-9-PLL/PVS | 2.65 | 32 | 16 ± 3 (D > L) | 3 ± 3 (D > L) |
| PEM-9-PEI-m/PVS | 2.76 | 40 | 2 ± 1 (L > D) | 30 ± 6 (L > D) |

integrals scale approximately linearly with the respective deposited amount because all prepared films in that report have thicknesses of $d < 50$ nm, which is shown in Table 1, and can therefore be classified as thin films due to Harrick (33). However, because of the different absorption coefficients $\varepsilon$ of IR bands, different bands show different absorbance amplitudes and cannot be directly compared in terms of the surface concentration. Knowing $\varepsilon$ or determination by, e.g., a concentration series, this would be possible (34) but is beyond the scope of this report. From the wavenumber maxima of the amide I and amide II bands, it can be concluded that PLL is predominantly in the α-helical conformation (25), which is due to the lack of electric repulsion and the formation of hydrogen bonds between the uncharged PLL repeating units at pH = 10 (35). The integrals of amide II, $\nu(SO_2)$, and $\nu$(OH) bands are plotted versus $z$ in Figure 3. Amide II and $\nu(SO_2)$ bands increase with the adsorption step $z$, showing a counterwise modulation feature: whenever PLL is immersed in a PEM with an outermost PSS layer, the amide II band due to PLL is increased, while the $\nu(SO_2)$ band is decreased and vice versa. From that, we conclude a partial release from a given outermost PEL layer by the oppositely charged one to form a soluble complex in the solution above the PEM. Such partial PEM erosion was already reported by Kovacevic et al. therein (36).

Furthermore, deposition data based on the integrals of diagnostic bands of the other PEMs PEI/PSS, PVP-R/PSS, PLL/PVS, and PEI-m/PVS were also analyzed. The modulation features of diagnostic bands were also present in their deposition. The integrals of $\nu(SO_2)$ bands and thicknesses of PEMs consisting of nine layers (PEM-9) are listed in Table 1. PLL/PVS forms a thicker film compared to PLL/PSS, presumably because of the higher molecuar weight of PVS (PSS, $M_w$ = 70 000 g/mol; PVS, $M_w$ = 300 000 g/mol). For the other PEMs, because of the different deposition conditions for these prepared PEMs, the influence of the types of PELs on the deposited amount could not be directly compared.

**2. Enantiospecific Interaction.** For the measurements related to enantiospecificity, the deposited PEMs were further stabilized by glutardialdehyde because in the deposition profiles indications for PEL release upon immersion of the oppositely charged one were obtained, as was described above. This treatment led to a partial cross-link formation between the amino groups of PEI and PLL and stabilized the PEM, respectively, within the highly entangled PEM internal phase. From immersion experiments with 1 M NaCl solutions, no loss of deposited PEM material was obtained, only if this procedure was performed (data not shown).

***2.1. Influence of the Chiral Probe Concentration.*** In Figure 4a, in situ ATR-FTIR spectra are shown that are due to the difference between the spectra of PEM-PLL/PSS in contact with L/D-GLU solutions of various concentrations (0.0012−0.05 M) and of this PEM in contact with pure water. These spectra reflect the sum amounts of bound and bulk L-GLU (solid line) and D-GLU (broken line) at PEM-PLL/PSS. An overlapped line shape in the spectral region between 1800 and 1460 $cm^{-1}$ was observed that is due to contributions of $\nu$(C═O) around 1710 $cm^{-1}$, $\nu(COO^-)$ around 1550 $cm^{-1}$, and $\delta(NRH_3^+)$ around 1600 and 1500 $cm^{-1}$ of car-

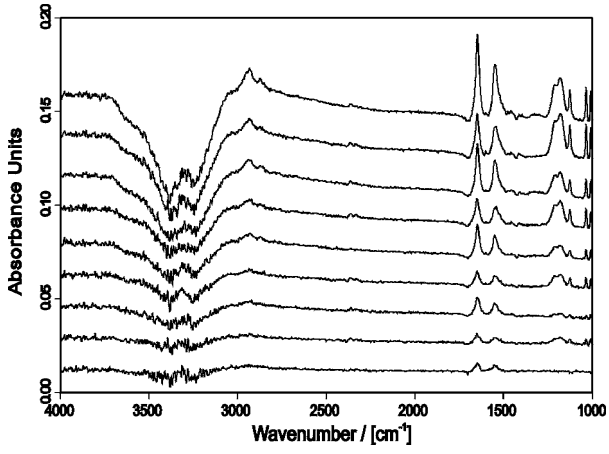


FIGURE 2. ATR-FTIR spectra on consecutive adsorption of PLL (0.005 M) and PSS (0.005 M) at pH = 10 onto the Ge-IRE. Spectra of PEM-1 (PLL) to PEM-9 (PLL) (from bottom to top) are shown.

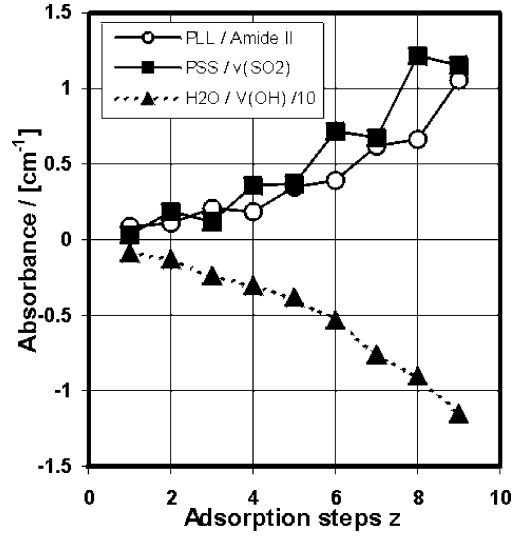


FIGURE 3. Deposition profile of PEM-PLL/PSS at pH = 10 rationalized by the integrated areas of the amide II band (PLL), $\nu(SO_2)$ band (PSS), and $\nu$(OH) band ($H_2O$) plotted versus the adsorption step $_z$.

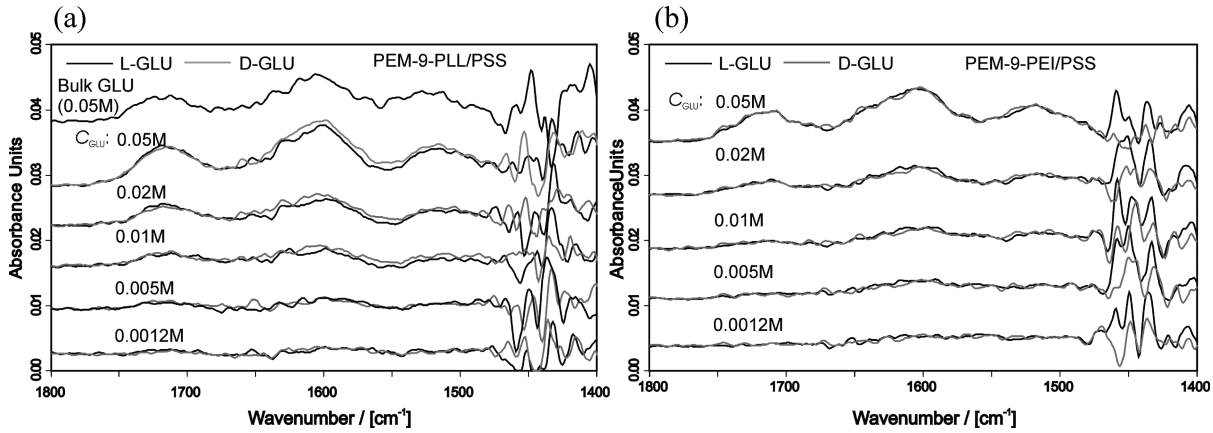


**FIGURE 4. ATR-FTIR difference spectra between (a) PEM-9-PLL/PSS and (b) PEM-9-PEI/PSS in contact with L/D-GLU solutions and the PEM in contact with Millipore water. The dark line is related to L-GLU and the gray line to D-GLU. The top spectrum in part a is due to a bulk solution of 0.05 M D-GLU on the naked Si-IRE surface.**

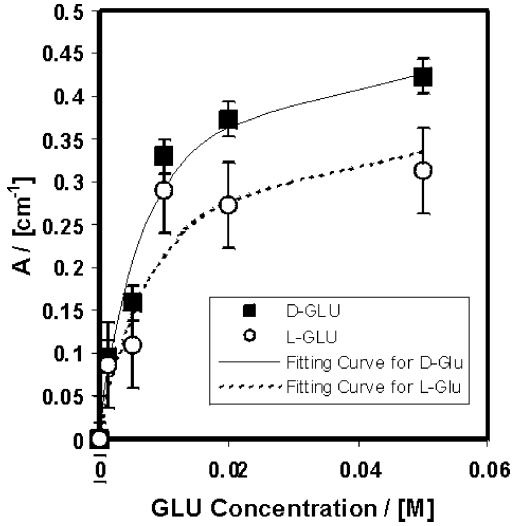


**FIGURE 5. Sum of the band integrals of corrected bound L- and D-GLU on PEM-9-PLL/PSS depending on $c_{GLU}$. The data were fitted by the analytical function given in eq 8.**

boxylic acid, carboxylate, and ammonium moieties, respectively, all more or less involved in the hydrogen bonding of one with another or to water. Among the whole GLU concentration range (0.0012−0.05 M), D-GLU shows the higher intensity in the spectra compared to L-GLU. When the 0.05 M bulk GLU spectrum (e.g., in contact with bare Si-IRE) and the spectrum of 0.05 M GLU in contact with PEM9-PLL/PSS were compared, it could be found that the contribution of bulk GLU dominates the original GLU spectrum. This is the reason why the bulk contribution must be corrected before evaluation of the enantiospecificty. Additionally, for comparison, ATR-FTIR spectra of L- and D-GLU interacting with nonchiral PEM-9-PEI/PSS are shown in Figure 4b, from which no spectral discrepancies and thus no enantiospecificity could be rationalized.

The sum of the band integrals of corrected bound L and D forms of GLU is plotted versus $c_{GLU}$ in Figure 5. The bound amount of GLU is calculated according to eq 7 using the integrals of the band (1800−1460 cm$^{-1}$; Figure 4) and the scaling factor SF = 0.898 (thickness $d$ = 15 nm). After an initial steep rise up to 0.02 M, the bound amount of GLU, as well as the difference between L- and D-GLU, saturates. At 0.05 M GLU, an enantiospecificity value of $S_E$ = 23% is obtained according to eq 1. The concentration-dependent data given in Figure 5 can be analyzed using a fitting function based on the Langmuir adsorption isotherm

$$A = \frac{A_0 c_{GLU}}{B + c_{GLU}} \quad (8)$$

$A_0$ and $B$ denote adjustable parameters. From $A_0$ and from $B = k_2/k_1$ the uptake and the ratio between the rate constants of forward and backward binding reactions, respectively, can be determined. Qualitatively, to characterize the enantiospecificity of a given PEM system for entire concentrations, $A_{0,D}$ and $A_{0,L}$ values (see the values above) could be taken to insert in eq 1 instead of $A_L$ and $A_D$ values. When the two concentration-dependent courses for D- and L-GLU for high $c_{GLU}$ are compared, a significant preference of D-GLU was obtained, which was supported quantitatively by the higher $A_0$ value for D-GLU ($A_{0,D}$ = 0.70 cm$^{-1}$) compared to that for L-GLU ($A_{0,L}$ = 0.56 cm$^{-1}$) based on eq 8. According to eq 1, the enantiospecificity of PEM-9-PLL/PSS was SE = 20% for GLU (D over L).

***2.2. Influence of the PEL Type.*** Different chiral polycations were combined with either PSS or PVS to check the influence of the PEL type on $S_E$. Table 1 summarizes the $S_E$ values of the studied PEM systems for L/D-GLU and L/D-ASC; the thicknesses of the PEM systems that are used for the corresponding SF calculation are also listed. First of all, the nonchiral PEM-PEI/PSS showed no enantiospecificity for the L or D forms: neither for GLU nor for ASC. However, PEMs containing PLL show significant values of $S_E$ = 21 ± 5% (PLL/PSS) and 16 ± 3% (PLL/PVS) for $c_{GLU}$ = 0.05 M (pH = 3.25) and of $S_E$ = 11 ± 5% (PLL/PSS) and 3 ± 3% (PLL/PVS) for $c_{ASC}$ = 0.05 M (pH = 4). Regarding the difference between PSS and PVS containing chiral PEMs, it seems that the aromatic groups of PSS play an additional role because of additional short-range interactions, resulting in higher enantiospecificities. For comparison to similar studies, Schlenoff (10) found around 3% enantiospecificity for a PEM, which was composed of poly(D-lysine) and poly(D-GLU), toward L-ASC (preference of the L enantiomer over the D enantiomer). Finally, the system PEM-PEI-m/PVS resulted in the

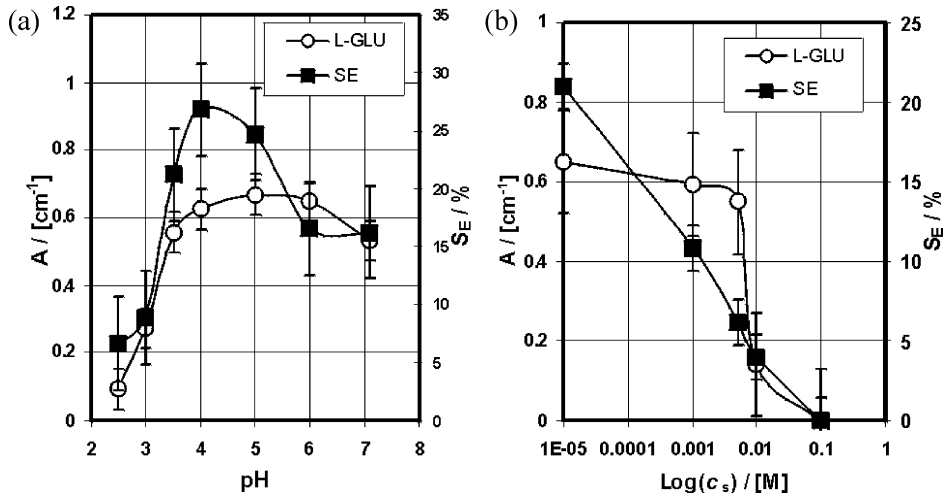


**FIGURE 6. (a) Bound amount of L-GLU on PEM-9-PLL/PSS and enantiospecificity $S_E$ values of PEM depending on the pH. (b) Bound amount of L-GLU on PEM-9-PLL/PSS and enantiospecificity $S_E$ values of the PEM depending on the NaCl concentration $c_s$.**

highest percent of enantiospecificity $S_E = 30 \pm 6\%$ with respect to L-ASC over D-ASC, while low enantiospecificity ($S_E = 2 \pm 1\%$) was found for GLU. Additionally, a similar trend was also found in PEM-PVP-R/PSS ($S_E = 2 \pm 1\%$ for GLU and $5 \pm 1\%$ for ASC).

Chiral discrimination is generally claimed to be based on weak interaction forces because the difference of the Gibbs free energy for chiral separation is ca. 240 J/mol at a chromatographic enantioselectivity $\alpha_{R,S} = 1.1$ (38). The weak interaction implies that the correct coordination of several individual forces is very complex. Such a coordination is mainly based on the structures of chiral selectors and probes. Hence, it can be found from Table 1 that the enantiospecificity highly depends on the combination of the chiral selector (PEM-PLL/polyanion or PEM-PEI-m/polyanion) and the chiral probe (GLU or ASC). Therefore, it might be speculated whether a PEM containing a homopolypeptide (PLL) shows higher enantiospecificity toward structurally related amino acids (GLU) compared to sugar derivatives (ASC), while a PEM containing sugar derivatives (PEM-m) shows higher enantiospecificity toward ASC than GLU. This speculation might be substantiated by a historical paper of Dagliesh (6), where the chiral recognition process was claimed to be based on a "three-point interaction mode", which means that at least three interaction pairs based on rather weak forces (van der Waals, diplole−dipole, hydrogen bonding, etc.) are formed between a chiral selector (SO) and a chiral selectand (SA).

***2.3. Influence of an Aqueous Medium. Influence of the pH.*** In our systems, electrostatic interaction between chiral SO (PEM) and SA (probe) is the dominant interaction type because both the outermost PEM (PLL) and probe (e.g., GLU) have charged units in contact to an aqueous solution. Because according to Dagliesh (6) chiral recognition is claimed to be based on multiple weak interaction forces, the role and control of the rather strong electrostatic force should be evaluated. Because the pH value is usually considered to be an important parameter for controlling the dissociation degree and thus the charge of weak PEL (PLL) and amino acids (GLU), we performed related studies.

Figure 6a shows the band integral of bound GLU, which is related to its sorbed amount, adsorbed from 0.05 M L-GLU solutions depending on the pH value ranging from pH = 2.5 to 7 at PEM-9-PLL/PSS. First, the bound amount of GLU increases with increasing pH, reaching a maximum at pH = 5. For pH > 5, the adsorbed amount decreases. This phenomenon can be explained by variation of the electrostatic interaction between PEM and GLU. The isoelectric points (IEPs) of GLU and lysine are 3.22 and 9.76, respectively. Hence, for pH < 3, both GLU and PLL had positive charges, so that few GLU could be bound onto the PEM because of repulsive electrostatic interaction. When the pH of the GLU solution was increased above its IEP, the carboxylic acid group (−COOH) and ammonium group ($NH_3^+$) of GLU were deprotonated and the charge sign was reversed from positive to negative, which was proved by the diminishing of the carboxylic acid band [$\nu$(C═O) at 1710 $cm^{-1}$] in the FTIR spectrum (data were not shown). Under such an attractive electrostatic interaction, the GLU molecules were strongly adsorbed by PEM. However, upon a further increase in the pH, another variation must be considered, which is the discharging of PLL upon reaching its IEP. Obviously, the balance between charging GLU and discharging PLL results in a maximum of the GLU bound amount at pH ∼ 5.

The corresponding enantiospecificities at different pH values are also plotted in Figure 6a. Similar to the sorbed amount (GLU band integral), $S_E$ first increases with increasing pH values (from pH = 2.5 to 4). After reaching the maximum value of $S_E = 26\%$ at pH ∼ 4, it starts to decrease. Because variations of the bound amount and enantiospecificity are similar (their maxima appear in the range of pH = 4−5), it could be speculated that the charge balance plays an important role in chiral discrimination on the PEM surface: a strong attractive electrostatic force between PEM and GLU results in a high enantiospecificity. This finding was unexpected because according to the classical opinion enantiospecificity and enantioselectivity are based on coordinated yet weak interaction forces between chiral SO and chiral SA (probe).

Presumably, besides the electrostatic attraction, contributions due to pH-dependent physical changes in the PEM might play a role. In that respect, the pH-mediated change in the charge state of PLL might also cause an increased swelling of the PEM. Highly charge-swollen chiral PEMs have a more open structure, resulting in a better accessibility of chiral groups, leading to higher enantiospecificity. Furthermore, no pH-dependent conformational changes of PLL were detected by ATR-FTIR spectroscopy because of the confined flexibility of PLL chains by cross-linking (37). Further experimental and theoretical studies must be performed in that direction.

***Influence of the Ionic Strength.*** Besides the pH variation mentioned above, it is known that the ionic strength also affects the charge density of weak PELs. Generally, in the presence of salt (e.g., NaCl), the charge of PEL, like PLL, can be screened by co-ions, which weakens the intramolecular and intermolecular electrostatic interaction. Figure 6b shows variation of the band integral due to the bound amount of L-GLU on PEM-9-PLL/PSS depending on the salt concentration $c_s$ (ionic strength). Obviously, with increasing $c_s$, the adsorbed amount of GLU decreases. Moreover, a jump between $c_s = 0.005$ and 0.01 M is observed. Taking only the co-ions into account and not GLU itself, this concentration increase corresponds to a decrease in the Debye screening length from $\lambda = 6$ nm (0.005 M) to $\lambda = 3$ nm (0.01 M). Obviously, this relatively small variation has a dramatic effect on the binding. However, Debye length variations at systems like PEM are complex and could influence the swelling state of the PEM, the charge state and conformation of the involved PEL, or the GLU net charge. Hence, we claim the occurrence but cannot give any explanation for this steplike concentration dependence of the binding.

Unlike the binding isotherm, for the dependence of enantiospecificity on log($c_s$) in Figure 6b, a linear curve was obtained. In other words, the highest ($S_E = 21\,\%$) and lowest ($S_E = 0\,\%$) enantiospecificity values are related to the lowest ($c_s = 0$ M) and highest ($c_s = 0.1$ M) ionic strengths. Again, the correlation between the electrostatic attraction and enantiospecificity was surprising because short-range interactions are claimed to be important for the enantiospecificity. However, analogous to the pH of $S_E$, the ionic strength might also cause changes in the accessibility of the outermost chiral PEM region. High ionic strength might also cause a more compact structure (39), with lower accessibility of the chiral PLL groups toward chiral GLU molecules. Obviously, in our case, both the pH and ionic strength influences suggest that long-range electrostatic interaction plays a crucial role in the chiral discrimination on chiral PEM. Two steps of chiral interaction might be speculated on: (1) Electrostatic interaction mediates the physical approach of chiral probes (GLU) over a long distance range to cause an enrichment in the vicinity of the chiral PEM surface presumably followed by diffusion into PEM. (2) Within this enriched phase, additional weak short-range interactions (van der Waals, hydrogen bonding, dipole−dipole, etc.) between a chiral probe and PEM might be formed. In other words, a strong "attractive" force like the electrostatic one is needed for the initial close approach of selector and selectand, after which further "multiple-point interactions" relevant for chiral recognition are accomplished, as was claimed by Dagliesh (6). These speculations might be supported by recent studies on the enantioselective exchange of electrostatically bound anionic fluorescent dyes by diluted L-GLU in comparison to D-GLU solutions at PLL-coated $TiO_2$ gel films (40). Interestingly, also in that work, the strong long-range attractive electrostatic force between PLL and L/D-GLU seems to serve as an initial close approach between chiral selector and selectand, followed by further selective weak short-range interactions.

**Table 2. Enantiospecific Binding of L/D-TRP at PEM-9-PLL/PSS Coated on Planar Si-IRE (ATR-FTIR) and Enantiospecific Permeation of L/D-TRP at PEM-9-PLL/PSS Coated on PTFE Membranes (UV−Vis)**

| | bound amount | | | | |
|---|---|---|---|---|---|
| modified substrate | $A_L$ [cm$^{-1}$] | $A_D$ [cm$^{-1}$] | | enantiospecificity $S_E$ | detecting method |
| Si-PEM-9-PLL/PSS | 0.46 | 0.52 | | 10 % | ATR-FTIR |
| | permeation coefficient | | | | |
| | $P_L$[cm$^2$ /s] | $P_D$[cm$^2$ /s] | | $P_L/P_D$ | |
| PTFE-PEM-9-PLL/PSS | $1.50 \times 10^{-8}$ | $1.31 \times 10^{-8}$ | | 1.14 | UV−vis |

**3. Enantiospecific Permeation.** Because of its potential application in chiral separation, in addition to the planar systems, the separation properties of porous membranes modified by identical PEM systems were studied. Related investigations on the modification of the PTFE substrate by the PEM can be found in the literature (41).

Herein, first results on the enantiospecific permeation of PTFE membranes modified by PEM-PLL/PSS-9 will briefly be reported. Because of the low sensitivity of GLU for UV−vis measurements and considerable long-term oxidation of ASC, L/D-TRP was used as the chiral probe in the enantiospecific permeation experiment. For a direct comparison with the permeation experiments, the interaction of L/D-TRP with PEM-PLL/PSS deposited on Si-IRE was also studied by ATR-FTIR. An enantiospecificity value of $S_E = 10\,\%$ was observed, which is included in Table 2. The lower $S_E$ values compared to those of L/D-GLU are presumably due to the low attractive electrostatic interaction between TRP and PEM, whose role was discussed above.

In detail concerning the permeation experiments, Figure 7 shows the dependence of the L/D-TRP concentration in the downstream compartment on the permeation time using a PEM-modified PTFE membrane. Obviously, the permeation rate of L-TRP is faster than that of D-TRP at PEM-9-PLL/PSS, from which different degrees of chiral interaction inside the membrane are concluded. A summary of the resulting enantiospecificities for the modified silica and PTFE substrates is given in Table 2. It reveals that chiral PEMs on completely different substrates (planar Si-IRE vs porous PTFE) possess similar chiral discrimination performances. Related studies by Frank (42) using grafted membranes for

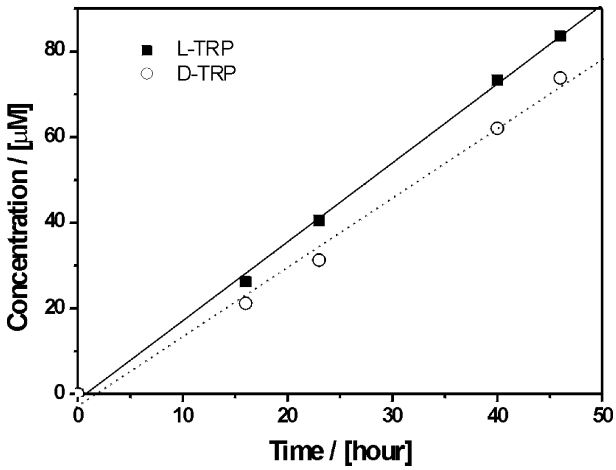


**FIGURE 7. Concentrations of L- and D-TRP in the downstream compartment of the permeation cell as a function of time for the PEM-9-PLL/PSS-modified PTFE membrane.**

enantiospecific permeation concluded that the chiral recognition found was mainly based on the α-helical conformation of PLL as the peptidic chiral selector.

## CONCLUSION

Chiral PEM deposition and their enantiospecific interaction to chiral model probes were studied using in situ ATR-FTIR spectroscopy. Three types of chiral PEM systems based on the chiral polycations PLL, PEI-m, and PVP-R in combination with either PSS or PVS were successfully deposited using consecutive adsorption. Additionally, a nonchiral PEM system composed of PEI/PSS was deposited. The nonchiral PEM did not show enantiospecificity toward the chiral probes L/D-GLU and L/D-ASC, whereas the chiral PEM of PLL/PSS and PLL/PVS showed significant enantiospecificity toward D-GLU over L-GLU and the chiral PEM of PEI-m/PSS revealed significant enantiospecificity toward D-ASC over L-ASC. Weak enantiospecificity was found between PLL/PSS and L/D-ASC, and no significant enantispecificity was found between PEI-m/PSS and L/D-GLU. The PEM of PLL/PSS showed increasing enantiospecificity upon an increase in the the attractive electrostatic force between PEM and GLU by pH or ionic strength variation. Further studies will address also neutral and cationic chiral probes. Additionally, we speculate on the enhanced accessibility of chiral groups in the PEM due to increased charge-mediated swelling. Identical PEM systems were used to modify the PTFE membranes and applied in permeation experiments, which resulted in significantly different retentions of L-TRP versus D-TRP. These studies contribute to a fundamental understanding of the chiral recognition and might help to find alternative concepts in preparative chiral separation technology.

**Acknowledgment.** Financial support from Deutsche Forschungsgemeinschaft (Grant DFG SFB 287 B5) is gratefully acknowledged.

### REFERENCES AND NOTES

(1) Rouhi, A. M. *Chem. Eng. News* **2003**, *81*, 45. *Chem. Eng. News* **2002**, *80*, 43.
(2) Roth, H. J.; Müller, C. E.; Folkers, G. *Stereochemie und Arzneistoffe*; Wissenschaft VG: Stuttgart, Germany, 1998.
(3) Pirkle, W. J. *J. Am. Chem. Soc.* **1966**, *88*, 1937–1943.
(4) Vinkovic, V.; Kontrec, D.; Sunjic, V.; Navarini, L.; Zanetti, F.; Azzolina, O. *Chirality* **2001**, *13*, 581–587.
(5) http://chrombook.merck.de/chrombook/index.jsp?j=0.
(6) Dagliesh, C. J. *J. Chem. Soc.* **1952**, 137–141.
(7) Fireman-Shoresh, S.; Avnir, D.; Marx, S. *Chem. Mater.* **2003**, *15*, 3607–3613.
(8) Huang, J.; Egan, V. M.; Guo, H.; Yoon, J. Y.; Briseno, A. L.; Rauda, I. E.; Garrell, R. L.; Knobler, C. M.; Zhou, F.; Kaner, R. B. *Adv. Mater.* **2003**, *15*, 1158–1161.
(9) Kaner, R. B.; Knobler, C. M.; Guo, H. Chiral recognition polymer and its use to separate enantiomers. U.S. Patent 6,265,615, 2001.
(10) Rmaile, H. H.; Schlenoff, J. B. *J. Am. Chem. Soc.* **2003**, *125*, 6602–6603.
(11) Sukhishvili, S. A.; Granick, S. *J. Am. Chem. Soc.* **2000**, *122*, 9550–9551.
(12) Xie, A. F.; Granick, S. *J. Am. Chem. Soc.* **2001**, *123*, 3175–3176.
(13) Boulmedais, F.; Schwinté, P.; Gergely, C.; Voegel, J. C.; Schaaf, P. *Langmuir* **2002**, *18*, 4523–4525.
(14) Schwinté, P.; Ball, V.; Szalontai, B.; Haikel, Y.; Voegel, J. C.; Schaaf, P. *Biomacromolecules* **2002**, *3*, 1135–1143.
(15) Debreczeny, M.; Ball, V.; Boulmedais, F.; Szalontai, B.; Voegel, J. C.; Schaaf, P. *J. Phys. Chem. B* **2003**, *107*, 12734–12739.
(16) Pilbat, A. M.; Ball, V.; Schaaf, P.; Voegel, J. C.; Szalontai, B. *Langmuir* **2006**, *22*, 5753–5759.
(17) Sukhishvili, S. A.; Dhinojwala, A.; Granick, S. *Langmuir* **1999**, *15*, 8474–8482.
(18) Kharlampieva, E.; Sukhishvili, S. A. *Macromolecules* **2003**, *36*, 9950–9956.
(19) Izumrudov, V.; Kharlampieva, E.; Sukhishvili, S. A. *Macromolecules* **2004**, *37*, 8400–8406.
(20) Sui, Z.; Schlenoff, J. B. *Langmuir* **2004**, *20*, 6026–6031.
(21) Jaber, J. A.; Schlenoff, J. B. *Langmuir* **2007**, *23*, 896–901.
(22) Schlenoff, J. B.; Rmaile, A. H.; Bucur, C. B. *J. Am. Chem. Soc.* **2008**, *130*, 13589–13597.
(23) Müller, M.; Rieser, T.; Lunkwitz, K.; Berwald, S.; Meier-Haack, J.; Jehnichen, D. *Macromol. Rapid Commun.* **1998**, *19*, 333–336.
(24) Müller, M.; Briššová, M.; Rieser, T.; Powers, A. C.; Lunkwitz, K. *Mater. Sci. Eng., C* **1999**, *8*, 167–173.
(25) Müller, M. *Biomacromolecules* **2001**, *2*, 262–269.
(26) Müller, M.; Kessler, B.; Lunkwitz, K. *J. Phys. Chem.* **2003**, *107* (32), 8189–8197.
(27) Müller, M. In *Handbook of Polyelectrolytes and Their Applications*; Tripathy, S. K., Kumar, J., Nalwa, H. S., Eds.; American Scientific Publishers: Valencia, CA, 2002; Vol. 1, p 293.
(28) Müller, M.; Grosse, I.; Jacobasch, H.-J.; Sams, P. *Tenside, Surfactants, Deterg.* **1998**, *35*, 354–359.
(29) Müller, M.; Rieser, T.; Dubin, P.; Lunkwitz, K. *Macromol. Rapid Commun.* **2001**, *22*, 390–395.
(30) Müller, M.; Kessler, B.; Houbenov, N.; Bohata, K.; Pientka, Z.; Brynda, E. *Biomacromolecules* **2006**, *7*, 1285–1294.
(31) Appelhans, D.; Zhong, Y.; Komber, H.; Friedel, P.; Oertel, U.; Scheler, U.; Morgner, N.; Kuckling, D.; Richter, S.; Seidel, J.; Brutschy, B.; Voit, B. *Macromol. Biosci.* **2007**, *7*, 373–383.
(32) Decher, G. *Science* **1997**, *277*, 1232–1237.
(33) Harrick, N. J. *Internal Reflection Spectroscopy*; Harrick Scientific Corp.: Ossining, NY, 1979.
(34) Fringeli, U. P. In *Encyclopedia of Spectroscopy and Spectrometry*; Lindon, J. C., Eds.; Accademic Press: London, 2000; p 58.
(35) Davidson, B.; Fasman, G. B. *Biochemistry* **1967**, *6*, 1616–1629.
(36) Kovacevic, D.; Van der Burgh, S.; de Keizer, A.; Cohen Stuart, M. A. *Langmuir* **2002**, *18*, 5607–5612.
(37) Ouyang, W. Dissertation, Technical University, Dresden, Germany, 2009.
(38) Marier, N. M.; Linder, W. In *Chirality in Drug Research*; Francotte, E., Linder, W., Eds.; Wiley-VCH Verlag GmbH & Co. KgaA: Weinheim, Germany, 2006; p 198.
(39) Dubas, S. T.; Schlenoff, J. B. *Langmuir* **2001**, *17*, 7725–7727.
(40) Paul, S.; Huang, J.; Ichinose, I. *New J. Chem.* **2005**, *29*, 1058–1063.
(41) Jaber, J. A.; Schlenoff, J. B. *J. Am. Chem. Soc.* **2006**, *128*, 2940–2947.
(42) Lee, N. H.; Frank, C. W. *Polymer* **2002**, *43*, 6255–6262.

AM900597C